Monthly Notices of the ROYAL ASTRONOMICAL SOCIETY

MNRAS **546,** 1–6 (2026) https://doi.org/10.1093/mnras/stag073
Advance Access publication 2026 January 20

Can GW231123 have a stellar origin?

Djuna Croon [1]★ Davide Gerosa [2,3] and Jeremy Sakstein [4]

[1]*Institute for Particle Physics Phenomenology, Department of Physics, Durham University, Durham DH1 3LE, UK*
[2]*Dipartimento di Fisica 'G. Occhialini', Universitá degli Studi di Milano-Bicocca, Piazza della Scienza 3, I-20126 Milano, Italy*
[3]*INFN, Sezione di Milano-Bicocca, Piazza della Scienza 3, I-20126 Milano, Italy*
[4]*Department of Physics & Astronomy, University of Hawai'i, Watanabe Hall, 2505 Correa Road, Honolulu, HI 96822, USA*

Accepted 2026 January 8. Received 2026 January 8; in original form 2025 October 22

ABSTRACT

The gravitational wave event GW231123 detected by the Laser Interferometer Gravitational-Wave Observatory (LIGO) interferometers during their fourth observing run features two black holes (BHs) with source-frame masses of 137^{+23}_{-18} and $101^{+22}_{-50}\,\mathrm{M}_\odot$ – in the range of the pair-instability BH mass gap predicted by standard stellar evolution theory. Both BHs are also inferred to be rapidly spinning ($\chi_1 \simeq 0.9$, $\chi_2 \simeq 0.8$). The primary object in GW231123 is the heaviest stellar mass BH detected to date, which, together with its extreme rotation, raises questions about its astrophysical origin. Accounting for the unusually large spin of ∼0.9 with hierarchical mergers requires some degree of fine-tuning. We investigate whether such a massive, highly spinning object could plausibly form from the collapse of a single rotating massive star. We simulate stars with an initial core mass of $160\,\mathrm{M}_\odot$ – sufficient to produce BH masses at the upper edge of the 90 per cent credible interval for m_1 in GW231123 – across a range of rotation rates and $^{12}\mathrm{C}(\alpha,\gamma)^{16}\mathrm{O}$ reaction rates. We allow for differential rotation to explore the high-spin regime. In this limit of weak angular momentum transport, we find that (i) rotation shifts the pair-instability mass gap to higher masses, introducing an important correlation between masses and spins in gravitational wave predictions, and (ii) highly spinning BHs with masses $\gtrsim 150\,\mathrm{M}_\odot$ can form above the mass gap. Our results suggest that the primary object of GW231123 may be the first directly observed BH that formed via direct core collapse following the photodisintegration instability.

Key words: gravitational waves – black hole mergers.

1 INTRODUCTION

On 2023 November 23, the LIGO Hanford and Livingston interferometers detected a short, ∼5-cycle signal consistent with the merger of two black holes (BHs) with source-frame masses

$$m_1 = 137^{+23}_{-18}\,\mathrm{M}_\odot, \quad m_2 = 101^{+22}_{-50}\,\mathrm{M}_\odot, \tag{1}$$

at redshift $z \approx 0.39$ (A. G. Abac et al. 2025). This event, dubbed GW231123, has total mass (190–265 $\mathrm{M}_\odot$) and spins ($\chi_1 \simeq 0.90^{+0.10}_{-0.19}$, $\chi_2 \simeq 0.80^{+0.20}_{-0.51}$), pushing into a regime where waveform systematics still need to be fully understood (A. G. Abac et al. 2025). Yet its high signal-to-noise ratio (∼22.5) and two-detector coincidence makes its identification robust. The high masses and spins distinguish GW231123 as a qualitatively new class of system, raising questions about its possible (astro)physical origin (see e.g. I. Bartos & Z. Haiman 2025; I. Cuceu et al. 2025; F. Kıroğlu, K. Kremer & F. A. Rasio 2025; Y.-J. Li et al. 2025; L. Paiella et al. 2025; J. Stegmann, A. Olejak & S. E. Mink 2025; A. Tanikawa et al. 2025; C. Yuan, Z.-C. Chen & L. Liu 2025).

Ostensibly, the combination of large masses and large spins in GW231123 could be explained by binaries formed through hierarchical mergers (for context, see D. Gerosa & M. Fishbach 2021 and references therein), and this appears to be a leading explanation in some of the recent literature (A. G. Abac et al. 2025; Y.-J. Li et al. 2025; L. Paiella et al. 2025; J. Stegmann et al. 2025). We argue that a hierarchical merger origin for GW23112's primary BH is unlikely; cf. I. Bartos & Z. Haiman (2025) for a similar argument. Hierarchical mergers in dense stellar environments produce a spin distribution that is sharply peaked at $\chi \sim 0.7$ (M. Fishbach, D. E. Holz & B. Farr 2017; D. Gerosa & E. Berti 2017), which matches the primary BH spin in GW231123 only near the lower edge of its 90 per cent credible interval. Spins of $\chi \sim 0.9$ are too large to be explained as merger remnants (D. Gerosa, N. Giacobbo & A. Vecchio 2021), requiring substantial fine-tuning of the progenitor binary (involving either a somewhat extreme mass ratio and/or mostly aligned spins). Motivated by these considerations, in this work we explore the possibility that the primary component of GW231123 could have formed from the direct collapse of a rotating massive star.

Stellar evolution theory predicts a 'pair-instability' black hole mass gap (BHMG) between approximately 60 and 130 $\mathrm{M}_\odot$, driven by electron-positron pair production in helium cores that powers (pulsational) pair-instability supernovae [hereafter (P)PISN] and completely disrupts stars with core masses up to ∼135 $\mathrm{M}_\odot$ (W. A. Fowler & F. Hoyle 1964; Z. Barkat, G. Rakavy & N. Sack 1967;

★ E-mail: djuna.l.croon@durham.ac.uk

G. Rakavy & G. Shaviv 1967; G. S. Fraley 1968; S. E. Woosley, A. Heger & T. A. Weaver 2002; M. Spera & M. Mapelli 2017; S. E. Woosley 2017; R. Farmer et al. 2019, 2020; S. E. Woosley & A. Heger 2021; E. Farag et al. 2022; A. K. Mehta et al. 2022; D. D. Hendriks et al. 2023). Various stellar parameters and other effects determine the location of the BHMG, most importantly the $^{12}C(\alpha,\gamma)^{16}O$ rate (K. Takahashi 2018; R. Farmer et al. 2019, 2020; J. Sakstein et al. 2020; E. Farag et al. 2022; A. K. Mehta et al. 2022), which can give variations of $\sim 47\,M_\odot$ (A. K. Mehta et al. 2022) in the location of the upper and lower edges of the BHMG.

If it had zero spin, the primary BH in GW231123 would likely lie above the BHMG unless the $^{12}C(\alpha,\gamma)^{16}O$ reaction rate were $\sim 3\sigma$ smaller than its median value (A. K. Mehta et al. 2022). However, this is based on simulations of (P)PISN that have neglected rotation, so this conclusion is unlikely to apply to GW231123 and its extremely high spins. Indeed, previous theoretical work (P. Marchant & T. Moriya 2020) has shown that rotation can raise the *lower* edge of the gap by ∼15 per cent (from 45.5 to 52.4 $M_\odot$). It is currently not known how rotation affects the *upper* edge of the BHMG.

A major uncertainty in modelling the rotational evolution of very massive stars is the efficiency of internal angular momentum transport. Much of the empirical support for strong core–envelope coupling, often modelled via the Spruit–Tayler (ST) dynamo, comes from low- and intermediate-mass stars. Its operation in very massive, radiation-dominated, and rapidly evolving stars, however, remains largely unconstrained observationally. The high spin inferred for the primary of GW231123 would be difficult to reconcile with standard stellar evolution models that enforce near-rigid rotation throughout the star's lifetime. Motivated by this tension, we explore an optimistic bracketing scenario in which internal angular momentum transport is inefficient, allowing the core to retain substantial rotation up to collapse. This assumption is not meant to be representative of typical massive stars, but rather to test whether the photodisintegration formation channel can remain viable even in the extreme case required by GW231123. Finally, we note that several studies have proposed evolutionary scenarios in which progenitors retain or regain substantial core rotation, including chemically homogeneous evolution (P. Marchant et al. 2016; S. E. Mink & I. Mandel 2016; S. A. Popa & S. E. Mink 2025), early envelope stripping in binaries (Y. Qin et al. 2018), and tidal spin-up (A. Olejak & K. Belczynski 2021). Our results provide a first indication of how pair-instability boundaries might be modified in such scenarios, independent of the detailed mechanism by which the core is spun up.

2 CORE COLLAPSE INSTABILITIES

The predicted BHMG is a direct result of the physics of pair instability, a well-studied effect (W. A. Fowler & F. Hoyle 1964; Z. Barkat et al. 1967; G. Rakavy & G. Shaviv 1967; G. S. Fraley 1968; S. E. Woosley et al. 2002; M. Spera & M. Mapelli 2017; S. E. Woosley 2017; K. Takahashi 2018; R. Farmer et al. 2019, 2020; S. E. Woosley & A. Heger 2021; E. Farag et al. 2022; A. K. Mehta et al. 2022; D. D. Hendriks et al. 2023) in massive post-main-sequence stars. At core temperatures $\gtrsim 10^9$ K, high-energy photons convert into non-relativistic electron–positron pairs, softening the equation of state such that the adiabatic index $\Gamma_1 < 4/3$, causing the core to contract, which in turn leads to explosive nuclear burning, primarily of oxygen. If the released nuclear energy exceeds the gravitational binding energy, the star is completely disrupted with no BH remnant. In a slightly lower mass range, the explosion is weaker and instead ejects the outer layers in pulses (a PPISN), removing mass until the remaining core collapses to a lighter BH. Above a critical helium core mass (∼130 $M_\odot$), stellar cores become so hot ($T_c \gtrsim 9\times10^9$ K) that high-energy photons begin to photodisintegrate iron-group nuclei into α-particles and free nucleons. This endothermic process decreases pressure support in the core (relative to continued nuclear burning), accelerating collapse – a phenomenon known as the photodisintegration instability. In this scenario, the star implodes directly to a BH, defining the upper edge of the BHMG.

Rotation impacts pair instability through two related mechanisms. First, the extra support provided by the centrifugal force results in lower temperatures at a given central density compared with non-rotating stars (P. Marchant & T. Moriya 2020; T. N. Huynh, E. Chatzopoulos & N. Zaman 2025). This shifts the star away from the regime where the effective adiabatic index drops below the critical value of 4/3 for dynamical instability. Secondly, if the core contracts while approximately conserving angular momentum, it spins up, further increasing centrifugal support during contraction, effectively lowering the critical value of Γ_1 for stability below 4/3. Together, these effects act to stabilize rapidly rotating stars against pair instability. It is presently not known what the effect on photodisintegration instability is.

In the absence of rotation, the onset and outcome of (P)PISN depend sensitively on the rates of core helium-burning reactions, particularly the competition between the triple-α process, which produces ^{12}C, and the subsequent $^{12}C(\alpha,\gamma)^{16}O$ channel. While uncertainties in both reaction rates affect the carbon-to-oxygen ratio, variations in the $^{12}C(\alpha,\gamma)^{16}O$ rate are the most important, dominating the shift in the carbon–oxygen core mass at which electron-positron pair production induces dynamical instability and thus altering the mass thresholds for (P)PISN events (K. Takahashi 2018; R. Farmer et al. 2019, 2020; E. Farag et al. 2022; A. K. Mehta et al. 2022). This rate is highly uncertain, with current experiments disagreeing by statistically significant amounts (R. J. deBoer et al. 2017). It is therefore standard practice to consider $\pm 3\sigma$ variations about the median between the various experimental constraints (T. Constantino et al. 2016; R. J. deBoer et al. 2017; K. Takahashi 2018; R. Farmer et al. 2019, 2020; M. T. Chidester, E. Farag & F. X. Timmes 2022; E. Farag et al. 2022; A. K. Mehta et al. 2022; M. T. Chidester, F. X. Timmes & E. Farag 2023; D. Croon & J. Sakstein 2025).

As the $^{12}C(\alpha,\gamma)^{16}O$ rate is raised, a larger fraction of ^{12}C is converted into ^{16}O during core helium burning. This higher oxygen abundance results in a stronger explosion, while the lower ^{12}C abundance implies less carbon is available to form a convective ^{12}C burning shell to counteract contraction (R. Farmer et al. 2020). Consequently, both the *lower* and *upper* edges of the mass gap move downward in tandem, preserving a nearly constant gap width of $\Delta M_{\rm BHMG} \approx 80^{+9}_{-5}\,M_\odot$ (A. K. Mehta et al. 2022). Across the full $\pm 3\sigma$ uncertainty in the reaction rate, the lower boundary shifts from $\sim 59^{+34}_{-13}\,M_\odot$ down to lighter values, while the upper boundary moves from $\sim 139^{+30}_{-14}\,M_\odot$ to correspondingly lower masses (A. K. Mehta et al. 2022).

3 SIMULATION SUITE

To assess the impact of rotation and nuclear physics on the boundaries of the pair-instability regime, we computed a grid of stellar models with an initial helium core mass of 160 $M_\odot$. This value was chosen such that, if no PISN occurs, the star can be

expected to form a BH with mass at the edge of the measured 90 per cent confidence for m_1 in GW231123. We vary the stellar rotation rate $\Omega/\Omega_{\rm crit}$ between 0 and 1 to capture the effects of increasing centrifugal support. The critical angular velocity,

$$\Omega_{\rm crit} \equiv \sqrt{\frac{(1-\Gamma)\,GM}{R_{\rm eq}^3}}\,, \tag{2}$$

is defined as the rotation rate at which the outward centrifugal acceleration at the stellar equator exactly balances the inward effective gravitational acceleration, where M is the gravitational mass, $R_{\rm eq}$ the equatorial radius, and $\Gamma \equiv L/L_{\rm Edd} = L\kappa/4\pi GMc$ is the local Eddington factor that accounts for radiation pressure. Additionally, we explore the variation of the rate of the temperature-dependent $^{12}{\rm C}(\alpha,\gamma)^{16}{\rm O}$ reaction over $\pm 3\sigma$ from its median rate $R_{\rm med}(T)$. Here, σ parametrizes the variation as $R_\sigma(T) = R_{\rm med}(T)\exp[\sigma\,\mu(T)]$, with $\mu(T)$ being the uncertainty at each temperature point, which is assumed to follow a log-normal distribution (R. J. deBoer et al. 2017; R. Farmer et al. 2020; A. K. Mehta et al. 2022).

Our simulations were performed using the stellar structure code MESA, version 15140 (B. Paxton et al. 2011; B. Paxton et al. 2013, 2015, 2018, 2019; A. S. Jermyn et al. 2023). While MESA is a one-dimensional code – meaning that it assumes spherical symmetry – it is capable of simulating rotating objects via the shellular approximation, where the radial coordinate r is replaced with the volume-equivalent radius of an isobar. A comprehensive description of rotation in MESA is provided in B. Paxton et al. (2019). Our code can be found in the paper's reproduction package (J. Sakstein 2025) at the following URL: https://zenodo.org/records/16898502.

We simulate 160 $\rm M_\odot$ rotating helium cores with metallicity $Z = 10^{-5}$ from the zero-age horizontal branch (ZAHB) to their end-state – either core collapse or disruption due to PISN – since their hydrogen envelopes are expected to be stripped by strong stellar winds or binary interactions, leaving behind bare helium cores that determine the subsequent evolution (A. Heger & S. E. Woosley 2002; J. J. Eldridge, R. G. Izzard & C. A. Tout 2008; K. Belczynski et al. 2016; S. E. Woosley 2017). Rotation is initialized at the ZAHB. Mass-loss to Wolf–Rayet winds are described, following the prescription of I. Brott et al. (2011), with a rotational enhancement described in B. Paxton et al. (2013). Stars that approach critical rotation are subject to additional mass losses, following B. Paxton et al. (2013) that remove angular momentum to keep them sub-critical. Convective mixing is implemented following the time-dependent formulation of P. Marchant et al. (2019); M. Renzo et al. (2020), which captures rapid changes in convective criteria during phases of dynamical instability but reduces to standard mixing length theory on long timescales. We take the mixing length efficiency to be $\alpha_{\rm MLT} = 2.0$. Convection is determined using the Ledoux criterion with semiconvection efficiency $\alpha_{\rm SC} = 1.0$. We employ exponential overshooting with $f = 0.01$. The switch from convective mixing to overshooting occurs at a distance $f_p H_P$ into the convective zone, with $f_p = 0.005$ and H_p being the pressure scale-height. We adopted the AGSS09 metal fractions (M. Asplund et al. 2009). These choices follow standard practice in recent studies of massive helium star evolution and pair-instability supernovae (D. Croon, S. D. McDermott & J. Sakstein 2020, 2021; J. Sakstein et al. 2020; M. C. Straight, J. Sakstein & E. J. Baxter 2020; J. Sakstein, D. Croon & S. D. McDermott 2022; D. Croon & J. Sakstein 2024), including the rotation prescription introduced by P. Marchant & T. Moriya (2020). We replaced the default MESA $^{12}{\rm C}(\alpha,\gamma)^{16}{\rm O}$ rate with the state-of-the-art tabulated values from A. K. Mehta et al. (2022), which sample the R. J. deBoer et al. (2017) rates; again consistent with contemporary works (E. Farag et al. 2022; A. K. Mehta et al. 2022; D. Croon & J. Sakstein 2025). Our resolution is higher than most MESA PPISN studies, following recent works that suggest such high resolutions are needed to fully resolve the core collapse-PPISN transition (E. Farag et al. 2022; A. K. Mehta et al. 2022; D. Croon & J. Sakstein 2025), although we note that a resolution study on the PISN-photodisintegration boundary has yet to be performed. Specifically, we set `delta_lgRho_cntr_limit = 0.001d0` and `max_dq = 5d-4` to enforce a smaller time-step and higher spatial resolution.

As noted above, our study is motivated by proposed evolutionary scenarios in which BH progenitor stars are rapidly rotating. For this reason, we do not include the ST dynamo (H. C. Spruit 2002), which is commonly invoked in stellar models to enforce near-rigid rotation through efficient angular momentum coupling between stellar layers (J. Fuller & L. Ma 2019; J. Fuller & W. Lu 2022). The physical validity and efficiency of this mechanism remain uncertain, and several studies have questioned whether the magnetic instabilities required to sustain the ST dynamo can operate under realistic stellar conditions (e.g. P. A. Denissenkov & M. Pinsonneault 2007; J. P. Zahn, A. S. Brun & S. Mathis 2007).

At the same time, it is widely recognized that some form of efficient angular momentum coupling must operate in stars in order to reproduce observational constraints, particularly those inferred from low- and intermediate-mass stellar remnants, such as the slow rotation of white dwarfs and neutron stars and the modest core–envelope differential rotation observed in evolved stars. Whether similarly efficient coupling operates in the very massive stars considered here, especially in the pair-instability regime, remains uncertain.

Models that adopt efficient angular momentum transport via the ST dynamo predict nearly non-rotating BHs (P. Marchant & T. Moriya 2020), which are difficult to reconcile with the high-component spins inferred for GW231123, potentially pointing to weaker internal angular momentum transport in its progenitor.[1] We therefore allow for differential rotation and spin retention in our models, which both enables high-spin remnants and directly impacts the onset of pair instability by shifting the upper edge of the mass gap to higher masses. Demonstrating that a rapidly spinning primary can still form above the mass gap strengthens the plausibility of a stellar-origin scenario involving photodisintegration collapse.

Some simulations feature spin parameters exceeding unity at core collapse. Although the BH may form with maximal spin, further accretion can reduce its spin if the added mass is not accompanied by sufficient angular momentum or if excess angular momentum is expelled by magnetohydrodynamic feedback (e.g. J. C. McKinney, A. Tchekhovskoy & R. D. Blandford 2012). To estimate the final spin of the BH, we adopt a version of the model developed by A. Batta & E. Ramirez-Ruiz (2019), consistent with previous work (P. Marchant & T. Moriya 2020). We assume that the innermost 3 $\rm M_\odot$ of the progenitor collapses promptly into a BH with maximal spin. We have explicitly verified that the results are insensitive to the size of this core; see Appendix A for more details. The remainder of the star is assumed to either fall directly

[1] We note that alternative interpretations suggest the nominal spin inference itself may be biased (A. Ray et al. 2025).

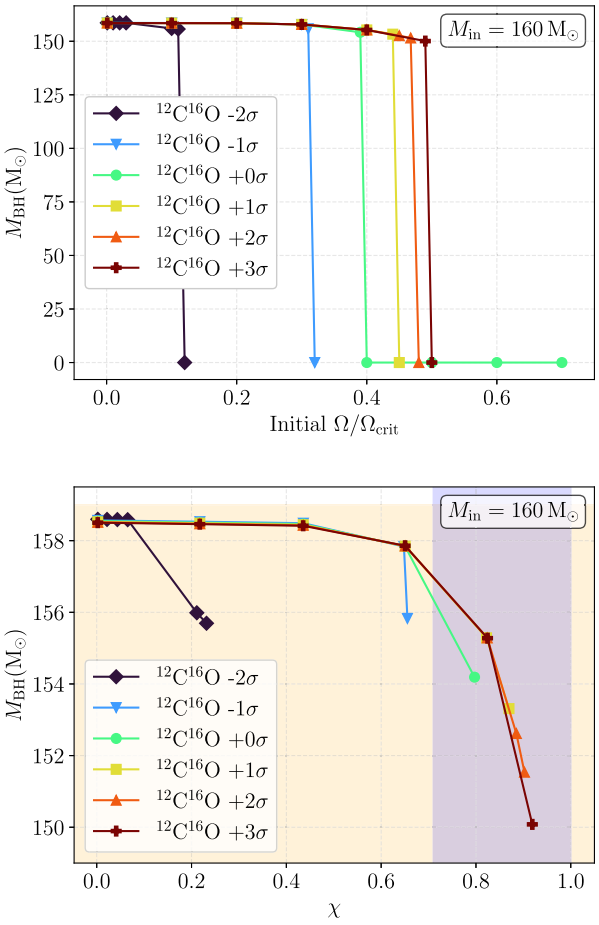

Figure 1. Final BH mass as a function of initial rotation, with initial helium core mass 160 $M_\odot$ for several values of the $^{12}C(\alpha,\gamma)^{16}O$ rate. The top panel shows results as a function of the initial stellar rotation Ω in units of the critical value $\Omega_{\rm crit}$; the bottom panel shows results as a function of the BH spin χ. Stars with faster rotation and smaller $^{12}C(\alpha,\gamma)^{16}O$ reaction rate undergo PISN and are not shown in the figure. The shaded contours indicate the 90 per cent credible intervals of the primary mass and spin in GW231123 (A. G. Abac et al. 2025).

into the BH or accrete through a disc, delivering additional mass and angular momentum. Accretion is regulated by feedback, ensuring that the final spin does not exceed the Kerr limit ($\chi \leq 1$).

4 RESULTS

4.1 Impact of rotation on the black hole mass gap

We show the results of our simulations in Fig. 1. The top panel shows the final BH mass as a function of the initial rotation rate $\Omega/\Omega_{\rm crit}$ for a 160 $M_\odot$ helium core, with $^{12}C(\alpha,\gamma)^{16}O$ reaction rates varied from -2σ to $+3\sigma$. The -3σ simulations produced PISN with no BH remnants for all $\Omega/\Omega_{\rm crit}$ (including zero) and are thus not shown. At low $\Omega/\Omega_{\rm crit}$, all models undergo direct collapse, yielding $M_{\rm BH} \approx 159\,{\rm M}_\odot$. At some critical rotation threshold $\Omega_{\rm PISN}$, the pair instability disrupts the star completely and no remnant is left. This threshold increases from $\Omega_{\rm PISN} \sim 0.1\,\Omega_{\rm crit}$ for the -2σ rate to $\Omega_{\rm PISN} \sim 0.5\,\Omega_{\rm crit}$ for the $+3\sigma$ rate, demonstrating that stronger carbon burning stabilizes the core against pair instability to higher rotation.

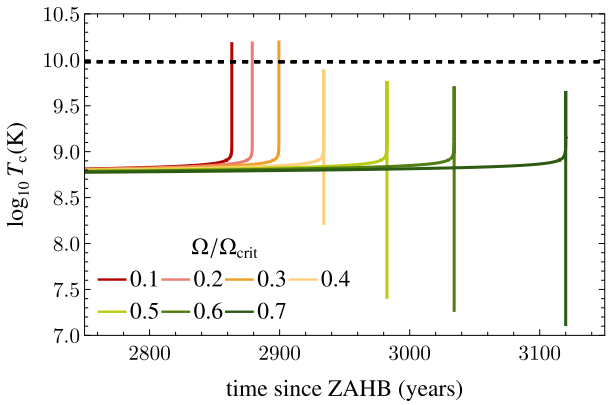

Figure 2. Central temperature $T_{\rm c}$ versus time since core helium depletion for the simulations described in text, with $M_{\rm in} = 160\,{\rm M}_\odot$ for the median $^{12}C(\alpha,\gamma)^{16}O$ rate. Non-rotating models reach higher core densities and temperatures, crossing into the regime where photodisintegration reactions lead to gravitational collapse, here assumed to be $T_{\rm c} = 9 \times 10^9$ K. Rotating models, by contrast, terminate at lower $T_{\rm c}$, thereby avoiding collapse and instead undergoing a PISN.

The bottom panel of Fig. 1 presents these same models in the BH spin–mass plane. Stars with a helium core mass of 160 $M_\odot$ cannot form BHs with a spin above a certain threshold, which depends on the $^{12}C(\alpha,\gamma)^{16}O$ reaction rate. In particular, BHs with spins and masses compatible with the 90 per cent confidence interval of the primary in GW231123 cannot be formed if the $^{12}C(\alpha,\gamma)^{16}O$ reaction rate is smaller than its measured median value.

As anticipated above, our results demonstrate that the photodisintegration boundary that marks the upper edge of the BHMG shifts to higher stellar masses in the presence of rapid rotation. As shown in Fig. 2, rotating stars reach lower core temperatures $T_{\rm c}$ before the onset of explosive oxygen burning leads to rapid expansion and a temperature drop. Thus, these stars avoid reaching the conditions required for photodisintegration-induced collapse and instead undergo PISN. For the median $^{12}C(\alpha,\gamma)^{16}O$ rate, we find that this occurs at $\Omega_{\rm PISN} \sim 0.4\,\Omega_{\rm crit}$.

4.2 Implications for GW231123

Our simulations imply that it is plausible to interpret GW231123's primary component ($m_1 \simeq 137\,{\rm M}_\odot$) as having formed via photodisintegration instability collapse, even with a rapidly rotating core in the absence of efficient angular momentum transport in the star. A similar claim was previously made (M. Fishbach & D. E. Holz 2020) for the primary BH in GW190521, the former high-mass record holder among GW events, although that interpretation depends strongly on the adopted prior distribution when analysing the underlying GW data.

In our models, the $^{12}C(\alpha,\gamma)^{16}O$ reaction rate needed to form GW231123's primary is both broad and realistic, ranging from the median to rates 3σ stronger. The upper end is compatible with previous hints that higher rates are needed to explain GW observations e.g. the 35 $M_\odot$ peak in the BH mass function (D. Croon & J. Sakstein 2025).

While our analysis has focused on the primary component of GW231123, it is worth briefly commenting on the secondary BH. The inferred mass posterior for the secondary is compatible with formation below the gap – the lower edge of the 90 per cent

credibility interval is $m_2 \sim 50\,M_\odot$. A natural possibility is therefore that GW231123 straddles the mass gap. This interpretation is supported from a GW data analysis perspective: in a massive event like GW231123, the total mass $m_1 + m_2$ is measured more accurately than either individual mass, which are consequently anticorrelated. If m_1 lies towards the upper end of its uncertainty range (placing it above the gap), then m_2 will lie towards the lower end of its range (and thus below the gap), a mechanism previously suggested to explain GW190521 by M. Fishbach & D. E. Holz (2020). As shown in this paper, this picture is further supported by the fact that rotation shifts the lower edge of the mass gap to higher masses. The secondary BH does not pose additional challenges to stellar-evolution models, although a dedicated evolutionary study of this object would certainly be worth pursuing.

5 OUTLOOK

GW231123 is a puzzling GW detection, with BHs that are among both the most massive and the most spinning detected so far. The primary BH, in particular, can reach $m_1 \sim 160\,M_\odot$ and is thus a promising candidate for a BH 'beyond the gap', with a progenitor subject to the photodisintegration instability.

We performed the first investigation of stars above the upper edge of the BHMG that includes both the effect of stellar rotation and variations in the critical $^{12}C(\alpha,\gamma)^{16}O$ nuclear-reaction rate. The main conclusion of this paper is that in the regime of weak angular momentum transport motivated by the spins of GW231123, it is possible that the primary component of GW231123 formed from direct stellar collapse.

An important assumption of this analysis is that we do not include the ST dynamo or other mechanisms that enforce strong angular momentum coupling. Efficient coupling would drive the core towards uniform rotation and produce nearly non-spinning BHs (e.g. P. Marchant & T. Moriya 2020; P. Marchant, P. Podsiadlowski & I. Mandel 2024), which would be inconsistent with the high spin inferred for GW231123 under current interpretations. Our results should therefore be understood as an exploration of the BHMG in the presence of rapidly rotating stellar cores, motivated by proposed scenarios in which massive stars can retain or regain substantial angular momentum.

Previous studies have shown that much of the information on population features often comes from a few highly informative events (S. M. Gaebel et al. 2019; E. J. Baxter et al. 2021; C. J. Moore & D. Gerosa 2021; R. Essick et al. 2022; M. Mancarella & D. Gerosa 2025). As was the case for GW190521 when analysing data from the first three LIGO/Virgo/KAGRA observing runs (R. Abbott et al. 2023), we anticipate that the exceptionally large masses and spins of GW231123 will play a major role in upcoming GW population constraints with O4 data. Accordingly, our conclusions that the large masses of GW231123 can be produced in combination with large spins through stellar evolution in the weak-coupling regime provide a foundation for population-level studies. We anticipate that it will be important for future GW population analyses to allow the stellar component to accommodate systems like GW231123, rather than imposing a hard cutoff at the BHMG. Fixing such a cutoff a priori could bias inferences towards exotic formation scenarios.

ACKNOWLEDGEMENTS

We thank Monica Colpi for discussions. DC was supported by Science and Technology Facilities Council (STFC) Grant No. ST/T001011/1. JS was supported by National Science Foundation (NSF) Grant No. 2207880. DG was supported by European Research Council (ERC) Starting Grant No. 945155–GWmining, Cariplo Foundation Grant No. 2021-0555, Ministry of University and Research (MUR) PRIN Grant No. 2022-Z9X4XS, Italian-French University (UIF/UFI) Grant No. 2025-C3-386, MUR Grant 'Progetto Dipartimenti di Eccellenza 2023–2027' (BiCoQ), Marie Skłodowska-Curie Actions (MSCA) Fellowship No. 101064542–StochRewind, MSCA Fellowship No. 101149270–ProtoBH, MUR Young Researchers Grant No. SOE2024-0000125, and the ICSC National Research Centre funded by NextGenerationEU. JS thanks the IPPP for hospitality and acknowledges an IPPP DIVA fellowship to support the visit. JS and DG thank the organizers of the International Congress of Basic Science (Beijing, 2025). Our simulations were run on the University of Hawai'i's high-performance supercomputer KOA. The technical support and advanced computing resources from University of Hawai'i Information Technology Services – Cyberinfrastructure, funded in part by the NSF MRI award No. 1920304, are gratefully acknowledged.

DATA AVAILABILITY

Our code can be found in the paper's reproduction package at the following URL: https://zenodo.org/records/16898502. Software used includes MESA version 15140, MESASDK version 20210401, GFORTRAN GCC version 9.2.0, GFORTRAN GCC version 9.2.0, JUPYTER NOTEBOOK version 6.4.12, PYTHON version 3.8.5, and MATHEMATICA via Wolfram version 14.2.

REFERENCES

Abac A. G. et al., 2025, ApJ, 993, L25
Abbott R. et al., 2023, Phys. Rev. X, 13, 011048
Asplund M., Grevesse N., Sauval A. J., Scott P., 2009, ARA&A, 47, 481
Barkat Z., Rakavy G., Sack N., 1967, Phys. Rev. Lett., 18, 379
Bartos I., Haiman Z., 2025, Astrophys. J. Lett., 996, L44
Batta A., Ramirez-Ruiz E., 2019, preprint ()
Baxter E. J., Croon D., McDermott S. D., Sakstein J., 2021, ApJ, 916, L16
Belczynski K., Holz D. E., Bulik T., O'Shaughnessy R., 2016, Nature, 534, 512
Brott I. et al., 2011, A&A, 530, A115
Chidester M. T., Farag E., Timmes F. X., 2022, ApJ, 935, 21
Chidester M. T., Timmes F. X., Farag E., 2023, ApJ, 954, 51
Constantino T., Campbell S. W., Lattanzio J. C., van Duijneveldt A., 2016, MNRAS, 456, 3866
Croon D., Sakstein J., 2024, Phys. Rev. D, 109, 103021
Croon D., Sakstein J., 2025, Phys. Rev. D, 112, 063053
Croon D., McDermott S. D., Sakstein J., 2020, Phys. Rev. D, 102, 115024
Croon D., McDermott S. D., Sakstein J., 2021, Phys. Dark Univ., 32, 100801
Cuceu I., Bizouard M. A., Christensen N., Sakellariadou M., 2026, Phys. Rev. D, 113, L021302
deBoer R. J. et al., 2017, Rev. Mod. Phys., 89, 035007
de Mink S. E., Mandel I., 2016, MNRAS, 460, 3545
Denissenkov P. A., Pinsonneault M., 2007, ApJ, 655, 1157
Eldridge J. J., Izzard R. G., Tout C. A., 2008, MNRAS, 384, 1109
Essick R., Farah A., Galaudage S., Talbot C., Fishbach M., Thrane E., Holz D. E., 2022, ApJ, 926, 34
Farag E., Renzo M., Farmer R., Chidester M. T., Timmes F. X., 2022, ApJ, 937, 112
Farmer R., Renzo M., de Mink S. E., Marchant P., Justham S., 2019, ApJ, 887, 53
Farmer R., Renzo M., de Mink S., Fishbach M., Justham S., 2020, ApJ, 902, L36
Fishbach M., Holz D. E., 2020, ApJ, 904, L26

Fishbach M., Holz D. E., Farr B., 2017, ApJ, 840, L24
Fowler W. A., Hoyle F., 1964, ApJS, 9, 201
Fraley G. S., 1968, Ap&SS, 2, 96
Fuller J., Lu W., 2022, MNRAS, 511, 3951
Fuller J., Ma L., 2019, ApJ, 881, L1
Gaebel S. M., Veitch J., Dent T., Farr W. M., 2019, MNRAS, 484, 4008
Gerosa D., Berti E., 2017, Phys. Rev. D, 95, 124046
Gerosa D., Fishbach M., 2021, Nat. Astron., 5, 749
Gerosa D., Giacobbo N., Vecchio A., 2021, ApJ, 915, 56
Heger A., Woosley S. E., 2002, ApJ, 567, 532
Hendriks D. D., van Son L. A. C., Renzo M., Izzard R. G., Farmer R., 2023, MNRAS, 526, 4130
Huynh T. N., Chatzopoulos E., Zaman N., 2025, ApJ, 991, 12
Jermyn A. S. et al., 2023, ApJS, 265, 15
Kıroğlu F., Kremer K., Rasio F. A., 2025, ApJ, 994, L37
Li Y.-J., Tang S.-P., Xue L.-Q., Fan Y.-Z., 2025, preprint ()
McKinney J. C., Tchekhovskoy A., Blandford R. D., 2012, MNRAS, 423, 3083
Mancarella M., Gerosa D., 2025, Phys. Rev. D, 111, 103012
Marchant P., Moriya T., 2020, A&A, 640, L18
Marchant P., Langer N., Podsiadlowski P., Tauris T. M., Moriya T. J., 2016, A&A, 588, A50
Marchant P., Renzo M., Farmer R., Pappas K. M., Taam R. E., De Mink S. E., Kalogera V., 2019, ApJ, 882, 36
Marchant P., Podsiadlowski P., Mandel I., 2024, A&A, 691, A339
Mehta A. K., Buonanno A., Gair J., Miller M. C., Farag E., deBoer R. J., Wiescher M., Timmes F. X., 2022, ApJ, 924, 39
Moore C. J., Gerosa D., 2021, Phys. Rev. D, 104, 083008
Olejak A., Belczynski K., 2021, ApJ, 921, L2
Paiella L., Ugolini C., Spera M., Branchesi M., Sedda M. A., 2025, ApJ, 994, L54
Paxton B., Bildsten L., Dotter A., Herwig F., Lesaffre P., Timmes F., 2011, ApJS, 192, 3
Paxton B. et al., 2013, ApJS, 208, 4
Paxton B. et al., 2015, ApJS, 220, 15
Paxton B. et al., 2018, ApJS, 234, 34
Paxton B. et al., 2019, ApJS, 243, 10
Popa S. A., de Mink S. E., 2025, Astrophys. J. Lett., 995, L76
Qin Y., Fragos T., Meynet G., Andrews J., Sørensen M., Song H. F., 2018, A&A, 616, A28
Rakavy G., Shaviv G., 1967, ApJ, 148, 803
Ray A., Banagiri S., Thrane E., Lasky P. D., 2025arXiv:2510.07228
Renzo M., Farmer R. J., Justham S., de Mink S. E., Götberg Y., Marchant P., 2020, MNRAS, 493, 4333
Sakstein J., 2025, Can stellar physics explain GW231123?. Zenodo.
Sakstein J., Croon D., McDermott S. D., Straight M. C., Baxter E. J., 2020, Phys. Rev. Lett., 125, 261105
Sakstein J., Croon D., McDermott S. D., 2022, Phys. Rev. D, 105, 095038
Spera M., Mapelli M., 2017, MNRAS, 470, 4739
Spruit H. C., 2002, A&A, 381, 923
Stegmann J., Olejak A., de Mink S. E., 2025, ApJ, 992, L26
Straight M. C., Sakstein J., Baxter E. J., 2020, Phys. Rev. D, 102, 124018
Takahashi K., 2018, ApJ, 863, 153
Tanikawa A., Liu S., Wu W., Fujii M. S., Wang L., 2025, preprint ()
Woosley S. E., 2017, ApJ, 836, 244
Woosley S. E., Heger A., 2021, ApJ, 912, L31
Woosley S. E., Heger A., Weaver T. A., 2002, Rev. Mod. Phys., 74, 1015
Yuan C., Chen Z.-C., Liu L., 2025, Phys. Rev. D, 112, L081306
Zahn J. P., Brun A. S., Mathis S., 2007, A&A, 474, 145

APPENDIX A: SENSITIVITY TO COLLAPSE DESCRIPTION

In Fig. A1, we examine the dependence of the final BH mass and dimensionless spin parameter χ on the initial rotation rate $\Omega/\Omega_{\rm crit}$ for two different choices of the prompt-collapse core mass, $M_{\rm cutoff} = 3$ and $5\,{\rm M}_\odot$. The left panel shows that across the full range $0.10 \leq \Omega/\Omega_{\rm crit} \leq 0.40$, the resulting BH mass varies by at most $\Delta M \lesssim 0.4\,{\rm M}_\odot$, while the right panel demonstrates that the spin parameter changes by less than $\Delta\chi \lesssim 0.02$. These small offsets confirm that our assumption of the mass of the inner core collapsing promptly has a negligible impact on the median-rate outcomes.

[t]

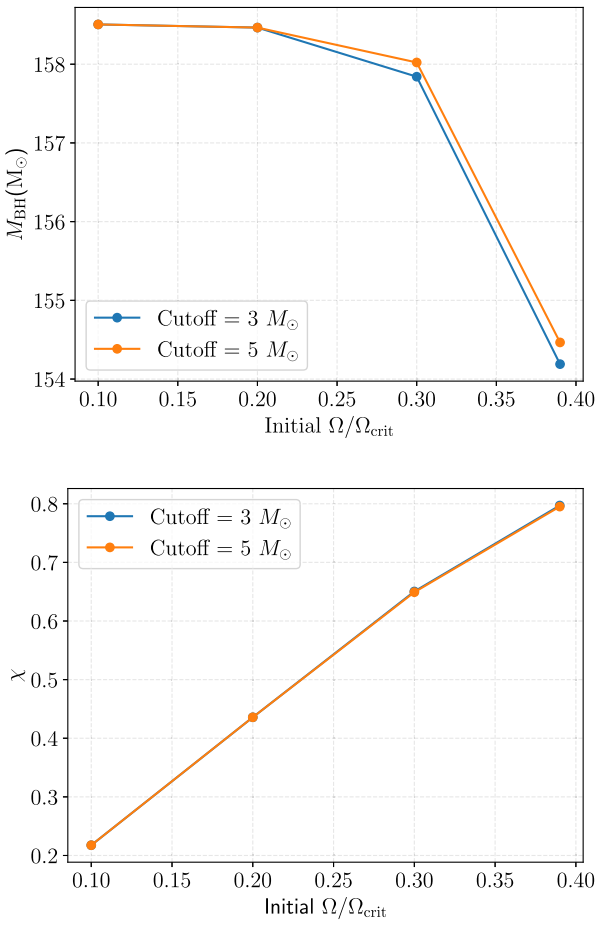

Figure A1. Final black-hole mass (*top*) and dimensionless spin parameter χ (*bottom*) as functions of the initial rotation rate $\Omega/\Omega_{\rm crit}$ for two choices of the prompt-collapse core mass threshold, $M_{\rm cutoff} = 3$ and $5\,{\rm M}_\odot$.

This paper has been typeset from a TEX/LATEX file prepared by the author.